Communication

Green Synthesis of MIL-88B(Cr) with the Co-Modulator of Nitric Acid and Acetic Acid

Fuzhi Li, Songfan Tang, Mingmin Li, Pengcheng Xiao, Mingliang Luo and Tian Zhao *

School of Packaging and Materials Engineering, Hunan University of Technology, Zhuzhou 412007, China; lifuzhi@hut.edu.cn (F.L.); mingminli2023@163.com (M.L.); xpc111294@163.com (P.X.); westbrook123666@163.com (M.L.)
* Correspondence: tian_zhao@hut.edu.cn

Abstract: MIL-88B(Cr) is a prototypical flexible chromium-based metal-organic framework (MOF), which possesses extremely strong water/thermal stability and excellent "swelling/breathing" ability. However, in previous studies, there have been very few reports on MIL-88B(Cr) due to unclear synthesis details. Here, we found that the pure MIL-88B(Cr) can be facile synthesized through a hydrothermal method with the co-use of nitric acid and acetic acid (molar ratio = 1:15). The obtained MIL-88B(Cr) was sufficiently characterized by diverse techniques to assure its high-level quality. This work emphasizes a future valuable approach to expanding the production of flexible Cr-based MOF.

Keywords: MIL-88B(Cr); flexible Cr-based MOF; co-modulator; green synthesis

1. Introduction

Metal organic frameworks (MOFs) are porous crystal coordination networks formed by connecting metal ions or their clusters through organic ligands [1–3]. In recent years, this type of material has received widespread attention due to its high porosity, demonstrating its enormous application potential in gas storage, separation, catalysis, thermal conversion, drug transportation, and other fields [3–10].

Flexible MOFs are unique in that they have the capacity to "breathe" or "swell" in response to different stimuli without causing permanent and irreversible damage to the frame structure [11]. This feature broadens the range of applications for MOFs in storage, sensing, and separation [12–17].

MIL-88 type MOFs have an **acs** network topology structure. It is reported that this type of material is mainly composed of metal elements (such as Fe, V, Cr, and NiIII/II) and a serial of terephthalate derivatives/analogues [18]. MIL-88 has an unparalleled "swelling/breathing" capability of up to 270% with 2,6-naphthalenedicarboxylic acid as the ligand in MIL-88C(Fe) [18]. This "swelling/breathing" ability is mainly caused by the introduction of the guest molecule, and the strong "swelling/breathing" ability enables MIL-88 MOFs to be used for important applications in separation/enrichment [19], sensing/analytical assays [20,21], drug delivery [22,23], and catalysis [24]. However, among all these applications related to MIL-88, only MIL-88(Fe) is widely used for application research, while MIL-88B(Cr) is rarely mentioned (where B specifically refers to its ligand being terephthalic acid, and its structure is shown in Figure 1) [25,26]. The main reason may be that the detailed experimental steps regarding MIL-88B(Cr) synthesis were not mentioned in the early original report [26], which makes the reports on MIL-88B(Cr) extremely scarce. It may seem like an oversight, but the implications are far-reaching. It is noteworthy that pyridine appears as a guest molecule in the molecular formula of MIL-88 regardless of the type of MIL-88 synthesis, which proves that pyridine was used in the original synthesis method. Thus, although it can be assumed that the conditions for the synthesis of MIL-88(Cr) are generally known, the actual absence of references to this compound in the literature indicates the urgent need for a simple and reproducible synthetic

method, preferably without the use of toxic pyridine. The potential interest in MIL-88 (Cr) stems from its high chemical stability, typical for chromium compounds, which would allow the use of the compound over a wider range of conditions. Therefore, it becomes useful and necessary to develop a simple and effective synthetic method that does not require the use of toxic pyridine to prepare MIL-88B(Cr).
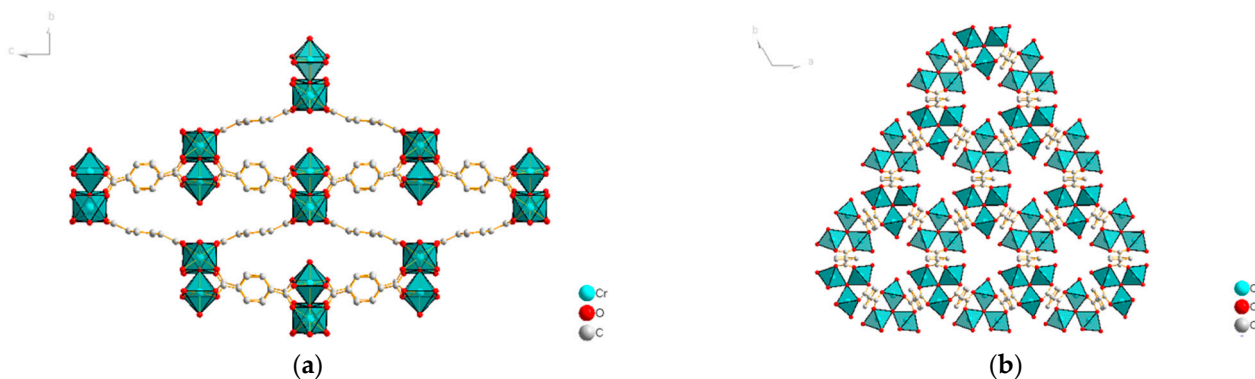

Figure 1. Schematic drawing of structure of the MIL-88(Cr) with the 'opened' form: (**a**) view along 100 direction, (**b**) view along 001 direction. The guest solvent molecules were not shown for clarity. (CSD-Refcode: YEDKOI) [26].

In our previous research, we were able to obtain pure MIL-88B(Cr) at 220 °C using a high concentration of benzoic acid as an additive, and chromium nitrate and terephthalic acid as raw materials by the conventional hydrothermal synthesis method [27]. Nevertheless, the residual benzoic acid in the structural pores of MIL-88B(Cr) synthesized with benzoic acid is difficult to remove, which limits its application. Here, we present a facile synthetic method for the preparation of pure MIL-88B(Cr) by co-using nitric acid and acetic acid with the appropriate molar ratio. The residual guest molecules (mainly HNO_3 and CH_3COOH) in the pores of MIL-88B(Cr) can be removed through simple treatment to achieve the 'close' structure.

2. Results and Discussion

In order to prepare MIL-88B(Cr), varied ratios of nitric acid: acetic acid were involved as modulators in the synthesis to obtain the optimal synthetic conditions. As the literature reported [28], the addition of equimolar nitric acid with respect to $Cr(NO_3)_3 \cdot 9H_2O$ in Cr-benzenedicarboxylate synthesis could largely increase the yield of the product, and this conclusion was proved multiple times to be correct by our group and others [29–32]. Thus, in this work, experiments with a constant amount of nitric acid (1 mmol) and different amounts of acetic acid (1 mmol, 5 mmol, 10 mmol and 15 mmol) were conducted, and they were named as A-1, A-2, A-3, and A-4, respectively.

The addition of nitric acid and acetic acid would significantly affect the particle size and the morphology of each sample. According to the scanning electron microscopic characterization, the A-X samples revealed dramatic morphological differences and particle size distributions (Figure 2). A-1 disclosed an octahedral shape (average particle size—400 nm) that indicated the characteristic morphology for MIL-101(Cr). A-2 showed obvious smaller crystals (~260 nm) compared with A-1, and its morphology mainly remained octahedral. While A-3 revealed two kinds of crystalline shape, one had octahedral particles and their average particle sizes further decreased to 140 nm, and the other had much bigger sharp-tipped rod-like crystals. Thus, undoubtedly, there were two kinds of different products that existed in A-3. Furthermore, when the ratio of nitric acid:acetic acid = 1:15 (A-4), all the products were rod-like crystals, which was in line with the features of MIL-88 type MOF [26,27]. Thus, the interesting effect of relatively drastic changes in crystallization results depending on the ratio of acetic acid and nitric acid was observed, with higher ratios of acetic acid and nitric acid favoring the MIL-88B(Cr) form.
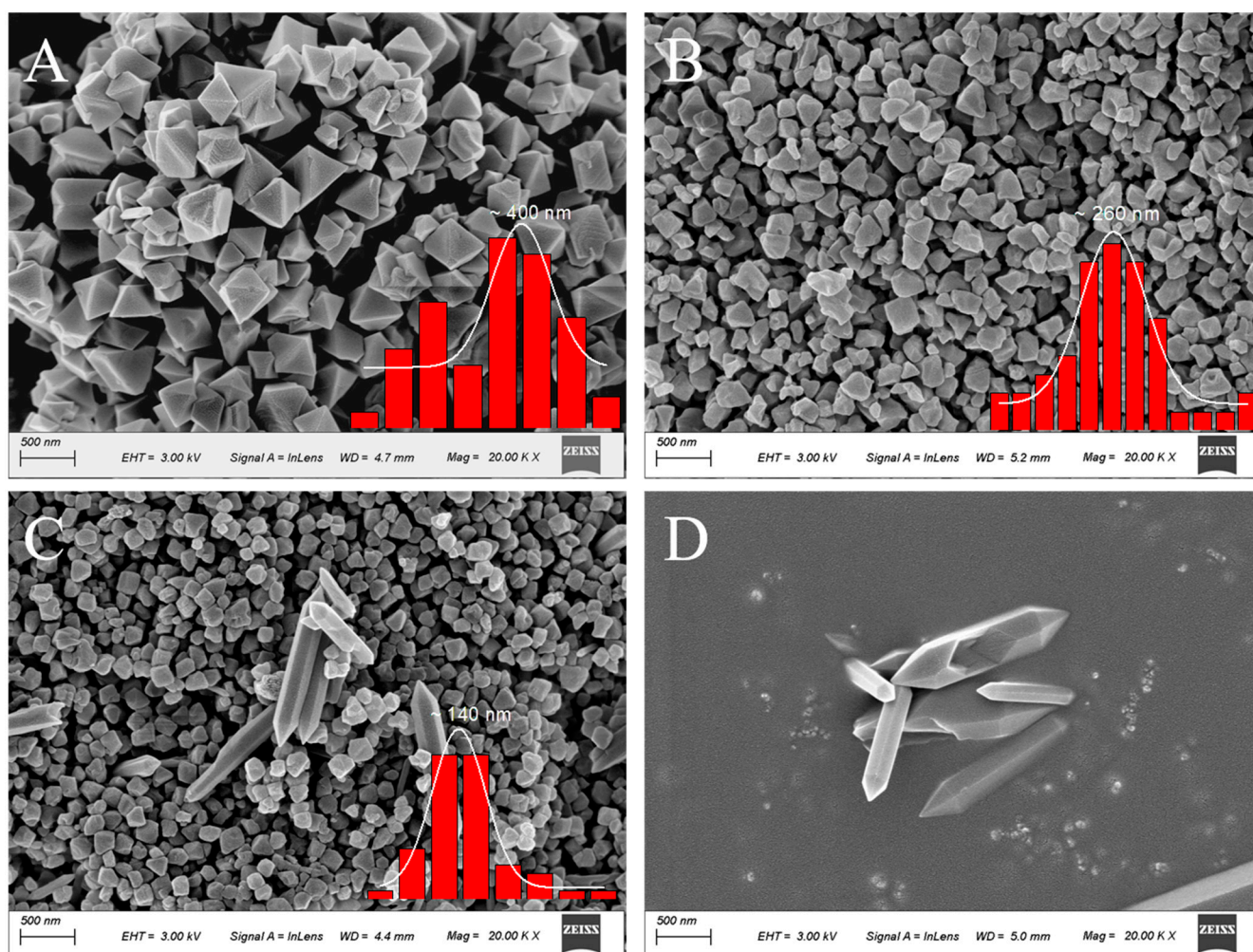
Figure 2. SEM images of (**A**) A-1, (**B**) A-2, (**C**) A-3, and (**D**) A-4, with the same scale bar. The insert image depicts the related particle size distribution, which was calculated using a Gaussian model.

The powder X-ray diffractograms (PXRDs) of A1~A4 were displayed in Figure 3. Apparently, the PXRDs of A-1 and A-2 showed very high consistency compared with the simulated MIL-101(Cr) pattern, which confirmed A-1 and A-2 were highly crystalline MIL-101(Cr) (Figure 3A). Although the PXRD of A-3 presented the characteristic peaks of MIL-101(Cr), a serial of peaks not matching the MIL-101(Cr) appeared beyond 20° (Figure 3A), which suggested another kind of crystal, and this result was highly in line with the microscopic characterization. While, for A-4, its PXRD was totally different from the simulated MIL-101(Cr) pattern, in contrast, its PXRD matched the MIL-88B(Cr) very well, which indicated that A-4 was a pure phase of MIL-88B(Cr) (Figure 3B).

The N_2 adsorption/desorption curves of A-1, A-2, A-3, and A-4 were shown in Figure 4, and the porosity information, including Brunauer–Emmett–Teller (BET) specific surface area, Langmuir specific surface area, and pore volume, are listed in Table 1. A-1 and A-2 revealed the typic Type I(b) N_2 sorption isotherms [33], and the second inflection point at relative pressure of $P/P_0 \approx 0.2$ referred to the two pore-cage sizes of MIL-101(Cr) [34]. Both A-1 and A-2 disclosed high porosity; their BET specific surface area could reach over 3300 $m^2\ g^{-1}$, while the S_{BET} of A-3 was much lower (only 1200 $m^2\ g^{-1}$). This could be attributed to the formation of MIL-88B(Cr) (Table 1). A-4 was pure MIL-88B(Cr), which had a "breathing" characteristic, and it was difficult to encourage its pores to open completely during the test, resulting in a very low porosity. Additionally, the N_2 sorption isotherms of A-4 were typical of Type I(a) because the pores of MIL-88B(Cr) belonged

to micropores, which was different from that of MIL-101(Cr) [33]. In summary, the N_2 adsorption/desorption measurements further validated our previous results.
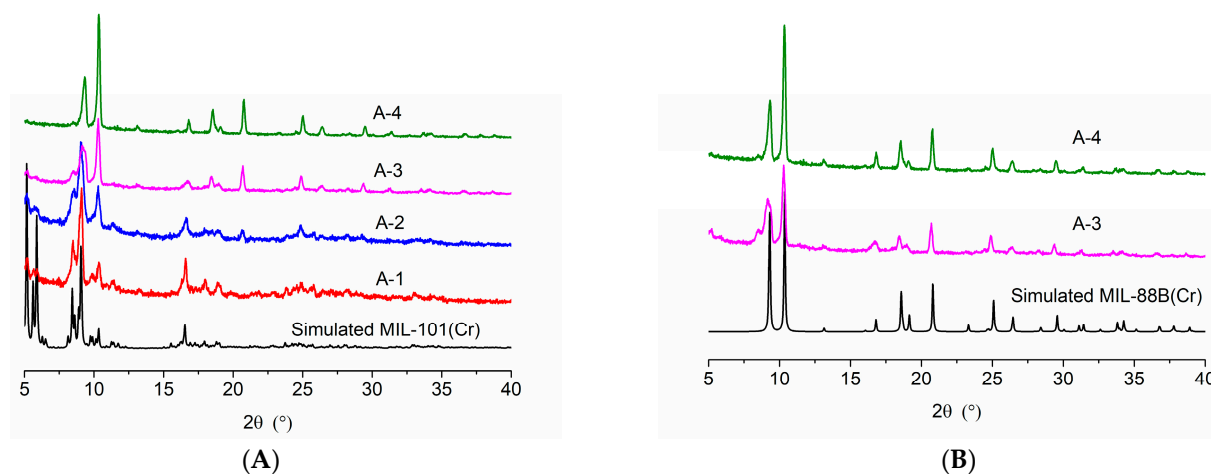
Figure 3. (**A**) The PXRDs of A1–A4 comparison with the simulated MIL-101(Cr) pattern. (**B**) The PXRDs of A-3 and A-4 compared to the simulated MIL-88B(Cr) pattern with the 'open' high-volume structure.
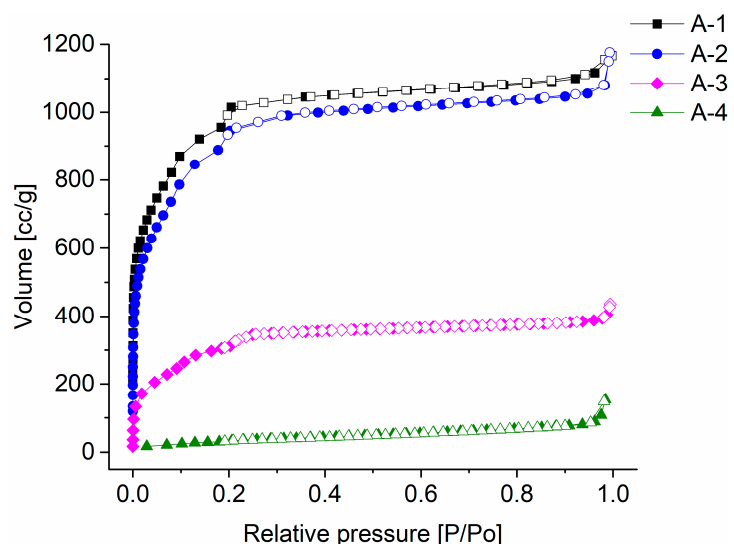
Figure 4. Nitrogen sorption isotherms of A-1–A-4.

Table 1. The porosity information and yields for Cr-benzenedicarboxylate with the different ratio of nitric acid:acetic acid (A1~A4).

Sample	MOF Type	Yield (%) [a]	S_{BET} (m^2 g^{-1}) [b]	$S_{Langmuir}$ (m^2 g^{-1})	V_{pore} (cm^3 g^{-1}) [c]
A-1	MIL-101	~74.3	3430	4620	2.03
A-2	MIL-101	~70.8	3310	4460	1.97
A-3	MIL101/MIL-88	~47.2	1200	1710	0.67
A-4	MIL-88	~20.6	130	180	0.32

[a] The yield is based on Cr. [b] S_{BET} is calculated by using N_2 adsorption isotherms at 77 K in the region of $0.05 < P/P_0 < 0.2$ for data points with an estimated standard deviation of ± 50 m^2 g^{-1}. [c] V_{pore} is calculated from N_2 sorption isotherms at 77 K ($P/P_0 = 0.99$) for pores with ≤ 20 nm diameters.

In the previous work [27], though MIL-88B(Cr) could be formed by adding high doses of benzoic acid as a modulator, the yield of MIL-88B(Cr) was quite low (<5%), as well as the residual benzoic acid in the structural pores of MIL-88B(Cr) being hard to remove, something that greatly limited the preparation and application of MIL-88B(Cr). While, in

this work, the co-use of nitric acid and acetic acid in synthesis was significantly raised, the yield of the MIL-88B(Cr) (>20%), and the additive molecular HNO_3 and CH_3COOH, were quite easy to remove, which considerably reduced the difficulty of post-processing the product.

Undoubtedly, the ratio of acetic acid and nitric acid played a decisive role in the synthesis process. One possible explanation for this phenomenon was that the relatively low ratio of acetic acid and nitric acid inhibited Oswald ripening, which resulted in the generation of more nuclei and gave a smaller particle size MIL-101(Cr) (A-2) [4]. However, the situation was different when the addition of acetic acid was significant (A-4), when a large number of acetic acid molecules flooded the reaction system and acted as a templating agent-like effect, resulting in the generation of specific MOF structures, such as MIL-88B(Cr).

MIL-88B(Cr) is well-known to "swell" when exposed to polar solvents (e.g., MeOH) [26], which suggests that obvious PXRD pattern changes would occur when the polar solvents are trapped in the pores of MIL-88B(Cr). Thus, the synthesized MIL-88B(Cr) was soaked in MeOH to obtain a "swell" structure. And the incubation of the fabricated MIL-88B(Cr) in MeOH generated similar diffraction peaks, demonstrating the stretching of the flexible framework to introduce more solvent molecules, thus producing significant changes in the PXRD pattern (Figure 5A). The MeOH molecular in the pores of the framework (A-4) could be washed out when it was further incubated in water, and this obtained the same diffraction pattern as the as-synthesized material, indicating that this process was indeed reversible (Figure 5A). Our experimental outcomes were in good agreement with the results reported by Férey's group [18], which support our conclusion that pure MIL-88B(Cr) was formed. MIL-101(Cr) and MIL-88B(Cr) both had relatively high, but not the same, thermal stability and MIL-88B(Cr) had better thermal stability; we performed thermogravimetric analysis on all samples, and the results are shown in Figure 5B.
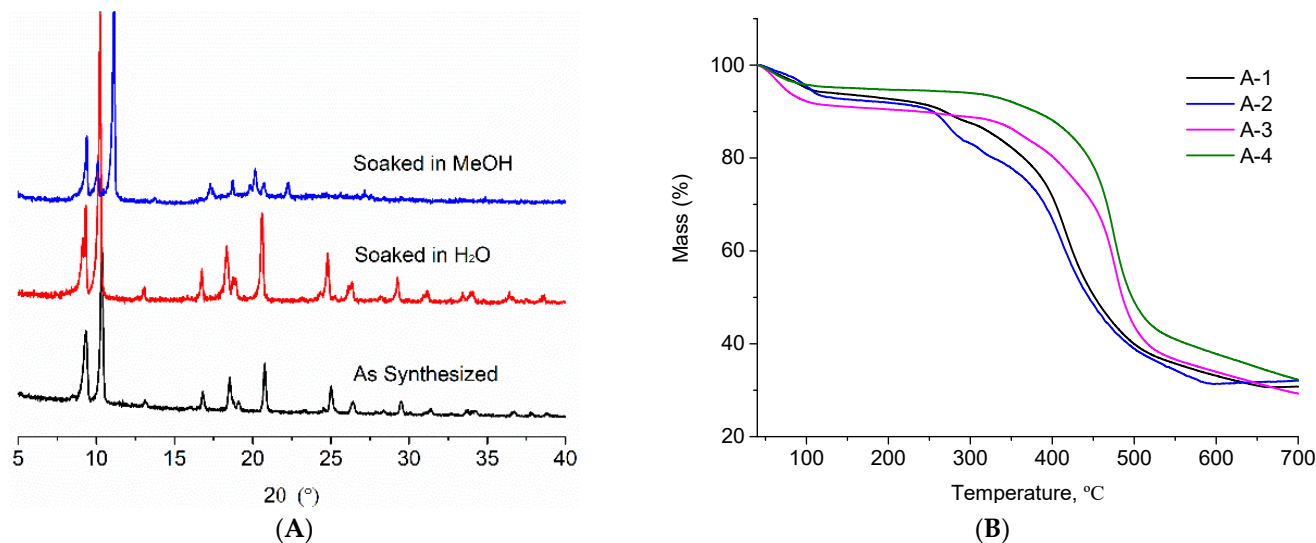
Figure 5. (**A**) The PXRD patterns of MIL-88B(Cr) (A-4) soaked in MeOH and H_2O to present its reversible breathing effect. (**B**) The TG curves of A-1–A-4.

3. Experimental

3.1. Materials and Reagents

Chromium(III) nitrate trihydrate (99.5%, AR), terephthalic acid (H_2BDC, 99%, AR), acetic acid (100%, AR), nitric acid (65 wt%, AR), and ethanol (99.7%, AR) were acquired from Sinopharm Chemical Reagent Co., Ltd. (Shanghai, China).

3.2. Synthesis of MIL-88B(Cr)

$Cr(NO_3)_3·9H_2O$ (400 mg, 1 mmol), H_2BDC (166 mg, 1 mmol), HNO_3 (1 mmol), and CH_3COOH (15 mmol) were stirred in deionized water and placed in a 20 mL autoclave.

The suspension was heated to 200 °C for 8 h. After the reaction was completed, the product was cooled naturally and washed twice with ethanol (1 h for each time). Then, the collected green solid was dried in a vacuum drying oven at 120 °C for 2 h before use.

3.3. Characterization

Powder X-ray diffraction (PXRD), using Ultima IV diffractometer (Rigaku, Tokyo, Japan), was conducted for sample analysis. The specific surface area and pore volume were measured using the NOVA 4200e specific surface analyzer (Quantachrome, Boynton Beach, FL, USA). Thermogravimetric analysis (TGA) was tested with a TGA/DSC 1/1100SF instrument (Mettler Toledo, Zurich, Switzerland). The morphologies of the samples were characterized using Zeiss Gemini 300 scanning electron microscopy (Zeiss, Jena, Germany).

4. Conclusions

MIL-101(Cr) and MIL-88B(Cr) could be flexibly synthesized using a hydrothermal method with the addition of nitric acid and acetic acid as modifiers. When the molar ratio of nitric acid and acetic acid added was 1:15, pure MIL-88B(Cr) could be obtained. This is a remarkably useful complement to the synthetic study of MIL-88B(Cr), and we have improved the methodology for the synthetic approach of forming MIL-88B(Cr) by avoiding the use of toxic organic compounds (e.g., Pyridine) during synthesis and treatment, which will lays the foundation for expanding the application of MIL-88B(Cr) in the future.

Author Contributions: Conceptualization, T.Z. and F.L.; methodology, F.L. and S.T.; formal analysis, S.T., M.L. (Mingmin LI) and P.X.; investigation, S.T. and M.L. (Mingliang Luo); resources, T.Z.; writing—original draft preparation, F.L., S.T. and T.Z.; writing—review and editing, T.Z.; supervision and funding acquisition, T.Z. All authors have read and agreed to the published version of the manuscript.

Data Availability Statement: Data is contained within the article.

Conflicts of Interest: The authors declare no conflict of interest.

References

1. Cai, G.; Yan, P.; Zhang, L.; Zhou, H.C.; Jiang, H.L. Metal-Organic Framework-Based Hierarchically Porous Materials: Synthesis and Applications. *Chem. Rev.* **2021**, *121*, 12278–12326. [CrossRef] [PubMed]
2. Theerthagiri, J.; Lee, S.J.; Murthy, A.P.; Madhavan, J.; Choi, M.Y. Fundamental aspects and recent advances in transition metal nitrides as electrocatalysts for hydrogen evolution reaction: A review. *Curr. Opin. Solid State Mater. Sci.* **2020**, *24*, 100805. [CrossRef]
3. Zorainy, M.Y.; Gar Alalm, M.; Kaliaguine, S.; Boffito, D.C. Revisiting the MIL-101 metal–organic framework: Design, synthesis, modifications, advances, and recent applications. *J. Mater. Chem. A* **2021**, *9*, 22159–22217. [CrossRef]
4. Zhao, T.; Li, S.; Xiao, Y.-X.; Janiak, C.; Chang, G.; Tian, G.; Yang, X.-Y. Template-free synthesis to micro-meso-macroporous hierarchy in nanostructured MIL-101(Cr) with enhanced catalytic activity. *Sci. China-Mater.* **2021**, *64*, 252–258. [CrossRef]
5. Hara, Y.; Sakaushi, K. Emergent electrochemical functions and future opportunities of hierarchically constructed metal-organic frameworks and covalent organic frameworks. *Nanoscale* **2021**, *13*, 6341–6356. [CrossRef] [PubMed]
6. Zhang, M.; Liu, Y. Enhancing the anti-corrosion performance of ZIF-8-based coatings via microstructural optimization. *New J. Chem.* **2020**, *44*, 2941–2946. [CrossRef]
7. Kubo, M.; Moriyama, R.; Shimada, M. Facile fabrication of HKUST-1 nanocomposites incorporating Fe3O4 and TiO2 nanoparticles by a spray-assisted synthetic process and their dye adsorption performances. *Microporous Mesoporous Mater.* **2019**, *280*, 227–235. [CrossRef]
8. Yu, R.; Wu, Z. High adsorption for ofloxacin and reusability by the use of ZIF-8 for wastewater treatment. *Microporous Mesoporous Mater.* **2020**, *308*, 110494. [CrossRef]

9. Theerthagiri, J.; Karuppasamy, K.; Lee, S.J.; Shwetharani, R.; Kim, H.-S.; Pasha, S.K.K.; Ashokkumar, M.; Choi, M.Y. Fundamentals and comprehensive insights on pulsed laser synthesis of advanced materials for diverse photo- and electrocatalytic applications. *Light Sci. Appl.* **2022**, *11*, 250. [CrossRef]

10. Chen, X.; Li, M.; Lin, M.; Lu, C.; Kumar, A.; Pan, Y.; Liu, J.; Peng, Y. Current and promising applications of Hf(iv)-based MOFs in clinical cancer therapy. *J. Mater. Chem. B* **2023**, *11*, 5693–5714. [CrossRef]

11. Férey, G.; Serre, C. Large breathing effects in three-dimensional porous hybrid matter: Facts, analyses, rules and consequences. *Chem. Soc. Rev.* **2009**, *38*, 1380–1399. [CrossRef] [PubMed]

12. Hamon, L.; Llewellyn, P.L.; Devic, T.; Ghoufi, A.; Clet, G.; Guillerm, V.; Pirngruber, G.D.; Maurin, G.; Serre, C.; Driver, G.; et al. Co-adsorption and Separation of CO_2-CH_4 Mixtures in the Highly Flexible MIL-53(Cr) MOF. *J. Am. Chem. Soc.* **2009**, *131*, 17490–17499. [CrossRef]

13. Jia, J.; Xu, F.; Long, Z.; Hou, X.; Sepaniak, M.J. Metal–organic framework MIL-53(Fe) for highly selective and ultrasensitive direct sensing of $MeHg^+$. *Chem. Commun.* **2013**, *49*, 4670–4672. [CrossRef] [PubMed]

14. Feng, L.; Wang, K.Y.; Day, G.S.; Ryder, M.R.; Zhou, H.C. Destruction of Metal-Organic Frameworks: Positive and Negative Aspects of Stability and Lability. *Chem. Rev.* **2020**, *120*, 13087–13133. [CrossRef] [PubMed]

15. Chen, J.; Zhang, Z.; Ma, J.; Nezamzadeh-Ejhieh, A.; Lu, C.; Pan, Y.; Liu, J.; Bai, Z. Current status and prospects of MOFs in controlled delivery of Pt anticancer drugs. *Dalton Trans.* **2023**, *52*, 6226–6238. [CrossRef]

16. Ke, F.; Pan, A.; Liu, J.; Liu, X.; Yuan, T.; Zhang, C.; Fu, G.; Peng, C.; Zhu, J.; Wan, X. Hierarchical camellia-like metal–organic frameworks via a bimetal competitive coordination combined with alkaline-assisted strategy for boosting selective fluoride removal from brick tea. *J. Colloid Interface Sci.* **2023**, *642*, 61–68. [CrossRef]

17. Chen, W.; Liu, M.; Yang, H.; Nezamzadeh-Ejhieh, A.; Lu, C.; Pan, Y.; Liu, J.; Bai, Z. Recent Advances of Fe(III)/Fe(II)-MPNs in Biomedical Applications. *Pharmaceutics* **2023**, *15*, 1323. [CrossRef]

18. Serre, C.; Mellot-Draznieks, C.; Surblé, S.; Audebrand, N.; Filinchuk, Y.; Férey, G. Role of Solvent-Host Interactions That Lead to Very Large Swelling of Hybrid Frameworks. *Science* **2007**, *315*, 1828–1831. [CrossRef]

19. He, J.; Zhang, Y.; Zhang, X.; Huang, Y. Highly efficient Fenton and enzyme-mimetic activities of NH2-MIL-88B(Fe) metal organic framework for methylene blue degradation. *Sci. Rep.* **2018**, *8*, 5159. [CrossRef]

20. Gao, C.; Zhu, H.; Chen, J.; Qiu, H. Facile synthesis of enzyme functional metal-organic framework for colorimetric detecting H2O2 and ascorbic acid. *Chin. Chem. Lett.* **2017**, *28*, 1006–1012. [CrossRef]

21. Zhang, Y.; Zhang, W.; Chen, K.; Yang, Q.; Hu, N.; Suo, Y.; Wang, J. Highly sensitive and selective colorimetric detection of glutathione via enhanced Fenton-like reaction of magnetic metal organic framework. *Sens. Actuators B Chem.* **2018**, *262*, 95–101. [CrossRef]

22. Horcajada, P.; Chalati, T.; Serre, C.; Gillet, B.; Sebrie, C.; Baati, T.; Eubank, J.F.; Heurtaux, D.; Clayette, P.; Kreuz, C.; et al. Porous metal–organic-framework nanoscale carriers as a potential platform for drug delivery and imaging. *Nat. Mater.* **2010**, *9*, 172–178. [CrossRef]

23. McKinlay, A.C.; Eubank, J.F.; Wuttke, S.; Xiao, B.; Wheatley, P.S.; Bazin, P.; Lavalley, J.C.; Daturi, M.; Vimont, A.; De Weireld, G.; et al. Nitric Oxide Adsorption and Delivery in Flexible MIL-88(Fe) Metal–Organic Frameworks. *Chem. Mater.* **2013**, *25*, 1592–1599. [CrossRef]

24. Rahmani, E.; Rahmani, M. Alkylation of benzene over Fe-based metal organic frameworks (MOFs) at low temperature condition. *Microporous Mesoporous Mater.* **2017**, *249*, 118–127. [CrossRef]

25. Serre, C.; Millange, F.; Surblé, S.; Férey, G. A Route to the Synthesis of Trivalent Transition-Metal Porous Carboxylates with Trimeric Secondary Building Units. *Angew. Chem. Int. Ed.* **2004**, *43*, 6285–6289. [CrossRef]

26. Surblé, S.; Serre, C.; Mellot-Draznieks, C.; Millange, F.; Férey, G. A new isoreticular class of metal-organic-frameworks with the MIL-88 topology. *Chem. Commun.* **2006**, 284–286. [CrossRef] [PubMed]

27. Yang, L.; Zhao, T.; Boldog, I.; Janiak, C.; Yang, X.Y.; Li, Q.; Zhou, Y.J.; Xia, Y.; Lai, D.W.; Liu, Y.J. Benzoic acid as a selector-modulator in the synthesis of MIL-88B(Cr) and nano-MIL-101(Cr). *Dalton Trans.* **2019**, *48*, 989–996. [CrossRef] [PubMed]

28. Zhao, T.; Jeremias, F.; Boldog, I.; Nguyen, B.; Henninger, S.K.; Janiak, C. High-yield, fluoride-free and large-scale synthesis of MIL-101(Cr). *Dalton Trans.* **2015**, *44*, 16791–16801. [CrossRef]

29. Zhao, T.; Li, S.-H.; Shen, L.; Wang, Y.; Yang, X.-Y. The sized controlled synthesis of MIL-101(Cr) with enhanced CO_2 adsorption property. *Inorg. Chem. Commun.* **2018**, *96*, 47–51. [CrossRef]

30. Zhao, T.; Zhu, H.; Dong, M. Comparison of Catalytic Activity of Chromium–Benzenedicarboxylate Metal–Organic Framework Based on Various Synthetic Approach. *Catalysts* **2020**, *10*, 318. [CrossRef]

31. Liu, X.-M.; Xie, L.-H.; Wu, Y. Efficient Propylene/Ethylene Separation in Highly Porous Metal-Organic Frameworks. *Materials* **2023**, *16*, 154. [CrossRef] [PubMed]

32. Moinfar, S.; Khodayari, A.; Abdulrahman, S.S.; Aghaei, A.; Sohrabnezhad, S.; Jamil, L.A. Development of a SPE/GC-MS method for the determination of organophosphorus pesticides in food samples using syringe filters packed by GNP/MIL-101(Cr) nanocomposite. *Food Chem.* **2022**, *371*, 130997. [CrossRef]

33.	Thommes, M.; Kaneko, K.; Neimark, A.V.; Olivier, J.P.; Rodriguez-Reinoso, F.; Rouquerol, J.; Sing, K.S.W. Physisorption of gases, with special reference to the evaluation of surface area and pore size distribution (IUPAC Technical Report). *Pure Appl. Chem.* **2015**, *87*, 1051–1069. [CrossRef]

34.	Ferey, G.; Mellot-Draznieks, C.; Serre, C.; Millange, F.; Dutour, J.; Surble, S.; Margiolaki, I. A chromium terephthalate-based solid with unusually large pore volumes and surface area. *Science* **2005**, *309*, 2040–2042. [CrossRef] [PubMed]